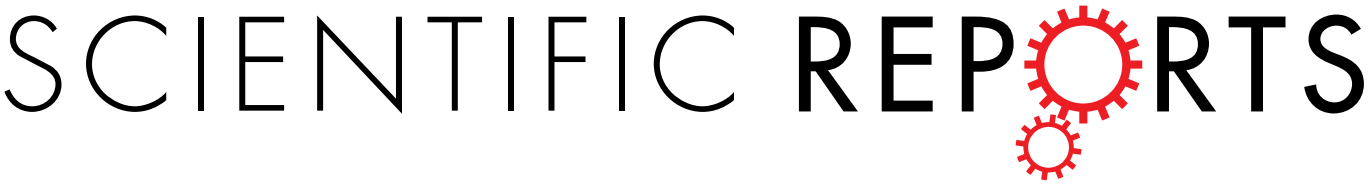

OPEN

Seasonal divergence in the interannual responses of Northern Hemisphere vegetation activity to variations in diurnal climate

Received: 10 March 2015
Accepted: 01 December 2015
Published: 11 January 2016

Xiuchen Wu[1,2,3], Hongyan Liu[4], Xiaoyan Li[1,2,3], Eryuan Liang[5], Pieter S.A. Beck[6] & Yongmei Huang[1,3]

Seasonal asymmetry in the interannual variations in the daytime and nighttime climate in the Northern Hemisphere (NH) is well documented, but its consequences for vegetation activity remain poorly understood. Here, we investigate the interannual responses of vegetation activity to variations of seasonal mean daytime and nighttime climate in NH (>30 °N) during the past decades using remote sensing retrievals, FLUXNET and tree ring data. Despite a generally significant and positive response of vegetation activity to seasonal mean maximum temperature (T_{max}) in ~22–25% of the boreal (>50 °N) NH between spring and autumn, spring-summer progressive water limitations appear to decouple vegetation activity from the mean summer T_{max}, particularly in climate zones with dry summers. Drought alleviation during autumn results in vegetation recovery from the marked warming-induced drought limitations observed in spring and summer across 24–26% of the temperate NH. Vegetation activity exhibits a pervasively negative correlation with the autumn mean minimum temperature, which is in contrast to the ambiguous patterns observed in spring and summer. Our findings provide new insights into how seasonal asymmetry in the interannual variations in the mean daytime and nighttime climate interacts with water limitations to produce spatiotemporally variable responses of vegetation growth.

The vegetation activity in temperate and cold regions is strongly controlled by climate, which is causing rapid changes in the vegetation activity in the Northern Hemisphere (NH) as the Earth warms[1–4]. Satellite observations, Earth system models and atmospheric inversions suggest that growing-season warming has increased the photosynthetic activity of the NH terrestrial vegetation during past decades[1,2,4] to a greater extent than other environmental processes (e.g., CO_2 and nitrogen fertilization)[5]. However, the responses of vegetation to climate warming are not uniform in space or time; covariation between the growing season temperature and vegetation activity varies regionally within the NH and appears to be weakening in many regions[6]. Simultaneously, mean daytime and nighttime warming during the growing-season produce different responses in vegetation productivity in the NH[3]. As spatial-temporal patterns of daytime and nighttime warming interact with extant seasonal hydrology, energy, and phenology cycles, stark differences in the vegetation responses are generated. However, such observed vegetation growth effects due to seasonal asymmetry in the interannual variations in the mean daytime and nighttime climate (VDNC)[7–9] and the underlying mechanisms that cause these effects to vary spatially remain poorly understood. Therefore, the effects of seasonal asymmetry in interannual variations in the mean diurnal climate on vegetation activity in the NH need to be better understood, especially because this asymmetry is predicted to increase[10].

[1]State Key Laboratory of Earth Processes and Resource Ecology, Beijing Normal University, Beijing, 100875, China. [2]Joint Center for Global Change Studies (JCGCS), Beijing, 100875, China. [3]College of Resources Science and Technology, Beijing Normal University, Beijing, 100875, China. [4]College of Urban and Environmental Science, Peking University, Beijing, 100871, China. [5]Key Laboratory of Tibetan Environment Changes and Land Surface Processes, Institute of Tibetan Plateau Research, Chinese Academy of Sciences, Beijing, 100085, China. [6]Forest Resources and Climate Unit, Institute for Environment and Sustainability (IES), Joint Research Centre (JRC), European Commission, Ispra, VA, Italy. Correspondence and requests for materials should be addressed to X.W. (email: xiuchen.wu@bnu.edu.cn)

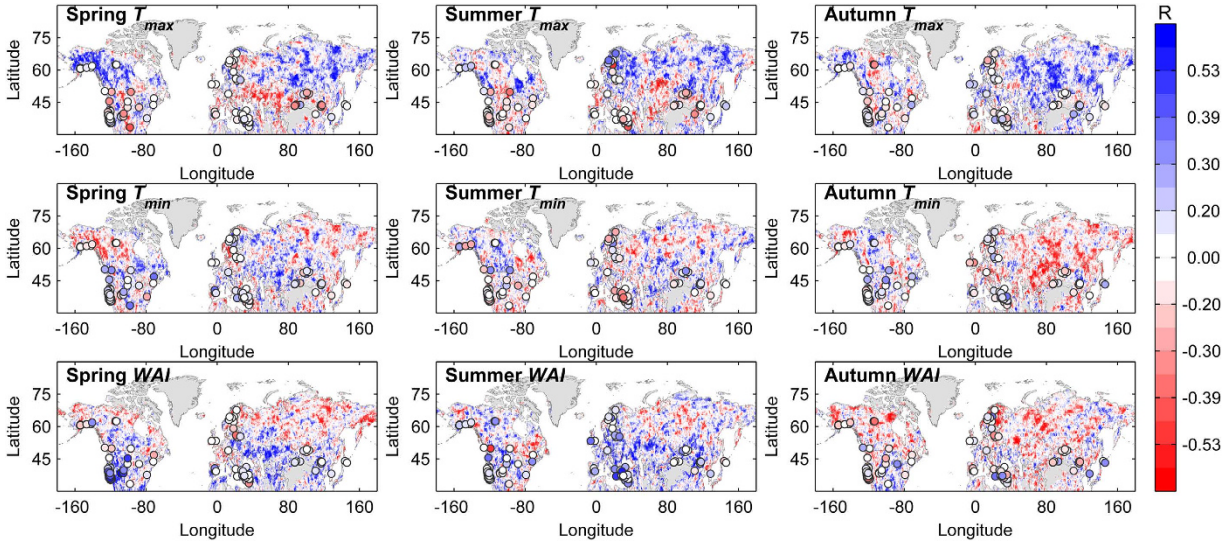

Figure 1. Spatial patterns of the interannual responses of the mean growing-season (April-October) NDVI and TRI to seasonal VDNC in the mid- and high-latitude NH. Spearman partial correlation coefficients between the mean growing-season NDVI ($NDVI_{GS}$) (during 1982–2008) and TRI (dots) (during 1950–2008, if available) as well as between the seasonal mean maximum temperature (T_{max}), mean minimum temperature (T_{min}) and water availability index (*WAI*) from spring to autumn are shown. $R = \pm 0.39$, $R = \pm 0.30$, and $R = \pm 0.20$ in the colorbar correspond to the 5%, 10% and 20% significance levels for the Spearman partial correlation between interannual variations of $NDVI_{GS}$ and seasonal mean climate, respectively. This figure is created by MATLAB (R2012b).

Asymmetry in the seasonal VDNC[11,12], together with other factors (e.g., land use changes[13]), could dramatically modify the seasonal thermo-hydrological patterns that govern land surface-climate feedbacks[14,15]. At middle and high latitudes in the NH, this asymmetry could hypothetically even modify the sign of biosphere-atmosphere feedbacks, which are known to be globally significant[15–17]. Therefore, in this study, we quantified the general patterns in the interannual responses of active vegetation growth (AVG, i.e., vegetation growth during the growing season) (for more detail, see Methods) at middle and high northern latitudes (>30°N) using 1) the satellite-derived Normalized Difference Vegetation Index (NDVI)[18,19] and the Fraction of Absorbed Photosynthetically Active Radiation (FAPAR)[20], 2) FLUXNET-based up-scaled gross primary productivity (GPP)[21], and 3) tree growth increments to the interannual variability (IAV) of seasonal mean maximum temperature (T_{max}), mean minimum temperature (T_{min}) and water availability index (WAI) during past decades (for more detail, see Methods).

Results

Covariance between vegetation activity and the seasonal mean T_{max}. Partial correlation analyses reveal a clear spatial pattern in the interannual responses of the mean growing-season (April-October) NDVI ($NDVI_{GS}$) to the IAV of the seasonal mean T_{max} during 1982–2008 (Fig. 1). $NDVI_{GS}$ generally exhibits a positive correlation with T_{max} in spring (April-May) (T^{sp}_{max}), summer (June-August) (T^{su}_{max}) and autumn (September-October) (T^{au}_{max}) in most (~60–70%) of the boreal NH (Figs 1 and 2a, Supplementary Table S1, Figs S1–S3), with statistically significant ($p < 0.10$) partial correlation coefficients ($R > 0.30$) in ~22–25% of boreal NH despite the great spatial variations in the responses (Fig. 1, Supplementary Table S2 and Figs S1, S3). Such response patterns of the AVG to the IAV of the seasonal mean T_{max} in the boreal NH are also supported by the analyses of mean growing-season FAPAR ($FAPAR_{GS}$) (Supplementary Figs S4a–c and S5a) and the results of independent ridge regression analyses (for more detail, see the supplementary text) of the relationships among $NDVI_{GS}$, $FAPAR_{GS}$ and the seasonal mean T_{max} during 1982–2008 (Supplementary Figs S6a–c and S7a–c). Coincidently, the ridge regression analyses reveal a generally positive interannual sensitivity of total growing-season GPP (GPP_{GS}) to seasonal mean T_{max} (γ_{GPP}, indicated by the coefficient of ridge regression) from spring to autumn in most (~51–89%) of the boreal NH (with statistical significance in ~20–62% of the boreal NH) despite large spatial variations (Fig. 3a, Supplementary Fig. S8a–c), with γ_{GPP} ranging from 36.5 ± 62.4 to 51.3 ± 88.7 g C m^{-2} yr^{-1} $°C^{-1}$ between seasons (Fig. 3a, Supplementary Fig. S8a–c).

By contrast, $NDVI_{GS}$ exhibits a significant ($p < 0.10$) negative correlation ($R < -0.30$) with the IAV of mean T^{sp}_{max} and T^{su}_{max} in ~13–16% of the temperate NH (<50 °N) during 1982–2008 (Fig. 1, Supplementary Table S1 and Fig. S1). The most prominent negative correlations are observed in the arid climate zones of the northern U.S.A., southern Eurasia and parts of the Mediterranean regions (Fig. 1, Supplementary Table S2 and Fig. S1), which are generally dominated by temperate grasslands, dry shrublands/forests or forest-grassland ecotones. Analyses of the relationships between the standard tree ring index (TRI) (during 1950–2008, if available), GPP_{GS}, $FAPAR_{GS}$ and the seasonal mean T_{max} confirm this pattern (Figs 1 and 3a, Supplementary Table S4, Figs S1, S4a–c, S5a, S7

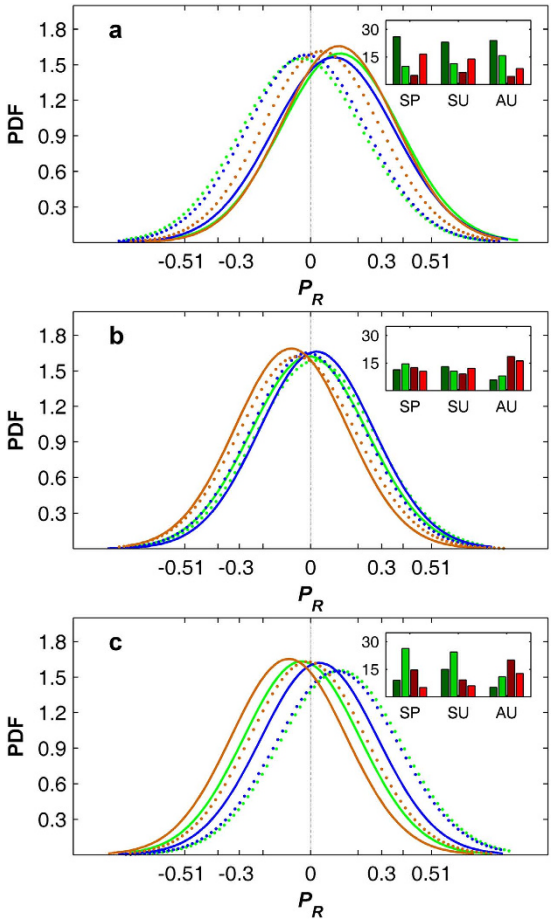

Figure 2. PDFs of the partial correlation coefficients between the mean growing-season (April-October) NDVI and the seasonal VDNC. PDFs of the partial correlation coefficients (P_R) between the mean growing-season NDVI and spring (green lines), summer (blue lines) and autumn (brown lines) maximum temperature (**a**), minimum temperature (**b**) and water availability index (**c**) in temperate (<50 °N, dotted lines) and boreal (≥50 °N, solid lines) regions of the NH. The percentages of the pixels that exhibit significant ($p < 0.10$) positive (green bars) and negative (red bars) correlations between the mean growing-season NDVI and spring (SP), summer (SU) and autumn (AU) maximum temperature, minimum temperature and WAI in temperate (light color) and boreal (dark color) regions are specified in the insets. The Spearman correlation coefficients $R \pm 0.51$ and ± 0.30 in the x axis tick label correspond to the 1% and 10% significance levels of Student's t-test, respectively.

and S8a–c). Partial correlation analyses reveal a generally negative correlation of TRI with mean T_{max}^{sp} and T_{max}^{su} in the temperate NH during 1950–2008 (if available) (with statistical significance for ~15% of samples) compared with a generally positive correlation in the boreal NH (with statistical significance for ~13% of samples) (Fig. 1, S1). Similarly, ridge regression reveals that GPP_{GS} in arid regions of the temperate NH (i.e., RegAR) exhibits a pervasively (~83–85% of RegAR) negative sensitivity to the IAV in T_{max}^{sp} and T_{max}^{su} during 1982–2008, with mean γ_{GPP} values of -24.9 ± 29.7 and -24.33 ± 28.5 g C m^{-2} yr^{-1} °C^{-1}, respectively (Fig. 3a, Supplementary Table S3).

Both partial correlation and ridge regression analyses of the relationships among $NDVI_{GS}$, $FAPAR_{GS}$, GPP_{GS}, TRI and the seasonal mean T_{max} consistently reveal a divergent response of the AVG to the IAV in the seasonal mean T_{max} for portions of the middle and high latitudes of the NH in two aspects. First, the AVG in parts of the boreal NH, especially regions with dry summer (i.e., RegAS) and warm temperate regions (e.g., the western and southeastern U.S.A.), responds differently to mean T_{max}^{sp} and T_{max}^{su} (Fig. 1, Supplementary Table S2, Table S3, Figs S1, S3, S4a,b and S6-S7a,b): The pervasive (~31%) significant positive correlation ($R > 0.30$) between $NDVI_{GS}$ and T_{max}^{sp} in RegAS tends to weaken (~9.1%) in summer (Fig. 1, Supplementary Table S2, Figs S1 and S3), whereas the $NDVI_{GS}$ maintains a significant positive correlation ($R > 0.30$) with the WAI (for ~15–17% of the samples) in both spring and summer (Fig. 1, Supplementary Table S2, Figs S1 and S2c). Eddy covariance observations in these regions support this notion of seasonal water limitation, indicating that GPP_{GS} responds positively to WAI in spring and summer during 1982–2008 (with spring and summer γ_{GPP} values of 1.2 ± 1.7 and 0.9 ± 1.8 g C m^{-2} yr^{-1} mm^{-1}, respectively, in RegAS) (Fig. 3c, Supplementary Table S3, Figs S8g,h,S9g,h and S10). In addition to the regions with dry summers in the boreal NH, GPP_{GS} in certain parts of the temperate NH also exhibits divergent

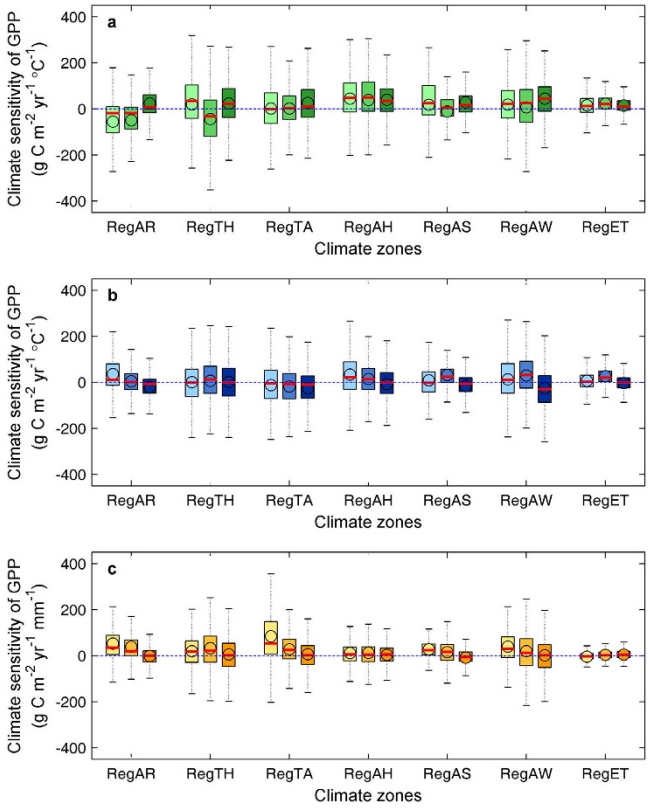

Figure 3. Interannual sensitivity of the growing-season (April-October) GPP to the seasonal VDNC in different climate zones. The sensitivity of the growing-season GPP to spring (light color), summer (medium color) and autumn (dark color) maximum temperature, minimum temperature and WAI in different climate zones are shown in panels a-c, respectively. The circles and short red lines in each box indicate the mean and median values, respectively, of the sensitivity of the growing-season GPP to the seasonal VDNC. The dashed lines and filled areas in each box represent the 5th to 95th and 25th to75th percentiles, respectively, of the sensitivity of the growing-season GPP to the seasonal VDNC. Seven major climate zones based on the Köppen–Geiger climate classification were considered in this study: RegAR (arid region, grouping of BWk, BWh, BSk, BSh), RegTH (temperate humid region, grouping of Cfa, Cfb, and Cfc), RegTA (temperate dry region, grouping of Csa, Csb, Csc, Cwa, Cwb and Cwc), RegAH (cold humid region, grouping of Dfa, Dfb, Dfc, and Dfd), RegAS (cold summer dry region, grouping of Dsa, Dsb, Dsc, and, Dsd), RegAW (cold winter dry region, grouping of Dwa, Dwb, Dwc, and, Dwd), and RegET (polar tundra, ET).

interannual sensitivity to T^{sp}_{max} and T^{su}_{max} (Fig. 3a, S9a,b and S10a), with γ_{GPP} values of 8.9 ± 22.1 in spring and -20.9 ± 43.6 g C m^{-2} yr^{-1} °C^{-1} in summer in RegTH (Fig. 3a, Supplementary Fig. S8a,b). At the same time, the TRI values in the temperate NH exhibit pervasive positive correlations with T^{sp}_{WAI} and T^{su}_{WAI} (with statistical significance at $p < 0.05$ level in ~14% and ~40% of samples, respectively) during 1950–2008 (Figs 1 and S1). Second, the interannual responses of the AVG to T^{au}_{max} diverge from the responses to T^{sp}_{max} and T^{su}_{max} in the majority of the temperate NH, especially in regions with drought limitations (e.g., RegAR and RegTA) (Supplementary Table S2). The $NDVI_{GS}$ exhibits a significant positive correlation ($R > 0.30$) with mean T^{au}_{max} in ~15–16% of the temperate NH but exhibits a significant positive correlation with T^{sp}_{max} and T^{su}_{max} in only ~<8% of that area (Figs 1 and 2a, Table S2, Fig. S1 and S2a).

Covariance between vegetation activity and the seasonal mean T_{min}. The interannual responses of the AVG in the middle and high latitudes of the NH to the mean spring and summer minimum temperatures (T^{sp}_{min} and T^{su}_{min}, respectively) are relatively ambiguous (Fig. 1, Supplementary Fig. S1, S2b, S4d,e, S5b and S6-S9d,e), yet the trends in $NDVI_{GS}$, GPP_{GS} and TRI indicate that the AVG responds positively to T^{sp}_{min} in certain parts of the temperate NH, particularly in arid regions (primarily in the central U.S.A. and southern Eurasia). The correlation with $NDVI_{GS}$ is statistically significant ($R > 0.30$, $p < 0.10$) in ~17.5% of these regions (Fig. 1, Supplementary Table S2, Fig. S1). Interestingly, such positive responses of the AVG to mean T_{min} tend to weaken from spring to summer in arid and temperate arid regions (Figs 1 and 3d,e, Supplementary Fig. S1) and instead become predominant in the high-latitude NH. Significant positive responses of $NDVI_{GS}$ and GPP_{GS} to T^{su}_{min} are observed in ~12–20% and ~23–64%, respectively, of cold regions and tundra (RegAH, RegAS and RegET) (Figs 1 and 3b, Supplementary Fig. S1, S3 and Table S2). Coincidently, the TRI exhibits a more pervasive positive correlation with T^{sp}_{min} (~15.8%) than with T^{su}_{min} (~7.9%) in the temperate NH (Fig. 1).

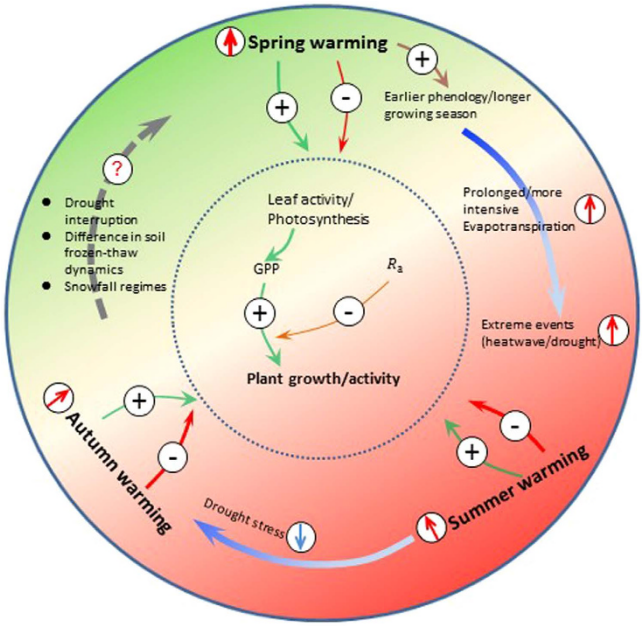

Figure 4. Conceptual diagram for water-mediated interannual responses of vegetation activity to the seasonal VDNC in the mid- and high-latitudinal NH. The green and red lines indicate the effects of seasonal variations in diurnal warming on plant photosynthesis/GPP and autotrophic respiration (R_a), respectively. The relative importance of the impacts and the relative warming rates between seasons are indicated by the line width (broader lines indicate greater importance). The blue arrow indicates the general soil water content following the transitions of seasons. The lighter blue color indicates more intense drought limitations for vegetation growth. The gray arrow indicates an unclear process. See also Reichstein *et al.* (2013) for the effects of extreme events on terrestrial ecosystems.

Contrary to the ambiguous relationships between AVG and T_{min}^{sp} and T_{min}^{su}, both $NDVI_{GS}$ and GPP_{GS} exhibit pervasively (60–63%) negative responses to T_{min}^{au} in most of the temperate and cold NH except in certain mountainous regions (e.g., the Rocky Mountains in western North America). Statistical significance is observed for $NDVI_{GS}$ in ~16% and ~18% of the temperate and boreal NH, respectively (Figs 1,2b and 3b, Supplementary Table S1, Table S3, Fig. S1 and Fig. S3). However, TRI data indicate a persistently positive rather than negative correlation with T_{min}^{au} during 1950–2008 (Fig. 1, Supplementary Fig. S1). Additionally, the observed divergent response patterns between AVG and seasonal VDNC are not susceptible to the arbitrary definitions of active growing seasons (Supplementary Fig. S11-S12) and selection of analysis periods (see Methods for details) (Supplementary Fig. S13).

Discussion

The results of both the partial correlation and ridge regression analyses demonstrate that the AVG in the boreal NH is generally temperature-limited: a warmer mean daytime temperature (i.e., T_{max}) during the active growing season can intuitively enhance the vegetation activity[1,2,4,22,23]. However, we have identified an obvious seasonally divergent response of the AVG to the IAV in seasonal mean T_{max} in parts of the high-latitude NH, especially in regions with dry summers. The AVG responds differently to T_{max}^{sp} and T_{max}^{su} (Fig. 1, Supplementary Table S2, Figs S1, S3, S4a,b and S5-S7a,b), and a pervasive (~31%) significant positive correlation is observed between $NDVI_{GS}$ and T_{max}^{sp} shading in summer (Fig. 1, Supplementary Table S2 and Fig. S3). In fact, the AVG in cold regions with dry summers is vulnerable to water stress under daytime warming, thereby resulting in seasonal drought[16,24,25], as confirmed by the close (~65.8–66%) positive coupling between the IAV in GPP_{GS} and the WAI during spring and summer. In addition to regions with dry summers in the boreal NH, the AVG in certain parts of the temperate NH also responds differently to mean T_{max}^{sp} and T_{max}^{su} (Fig. 1 Supplementary Figs S3, S6-S9a,b and S10a). The observed divergent responses of the AVG to T_{max}^{sp} and T_{max}^{su} in these regions may be partially attributed to the daytime warming-induced progressive drought from spring to summer, as revealed by a water balance equation and the relationships between the seasonal soil moisture and the VDNC during 1982–2008 (Fig. 4, Supplementary Figs S14-S16). TRI data reveal that tree growth in the temperate NH experiences continuous water limitations during spring and summer, as revealed by pervasive positive correlations of the TRI with T_{WAI}^{sp} and T_{WAI}^{su}. In fact, warmer daytime temperatures in spring can lead to an earlier spring phenology and greater photosynthesis[26,27], thereby enhancing vegetation growth as long as the soil water and atmospheric vapor pressure are sufficient. Conversely, if the increased warming rates during the early growing season are unmatched by water resources, the warmer temperatures can trigger a prolonged warming-induced drought, especially in regions that suffer seasonal drought limitations (e.g., RegAS and most regions in the temperate NH) (Fig. 4). Such cases of excessive soil water

stress or, more commonly, vapor pressure deficits (Supplementary Figs S14-S16, ref. Liu *et al.*, 2013[28]) can dramatically reduce vegetation growth and even negate springtime ecosystem carbon gains[16,25,29].

In addition to the divergent responses of the AVG to mean T_{max}^{sp} and T_{max}^{su} in parts of the mid- and high-latitude NH, the AVG responds differently to T_{max}^{au} than to T_{max}^{sp} and T_{max}^{su} across most of the temperate NH. Significant positive correlations between AVG and T_{max}^{au} are observed in nearly twice as many areas as those of T_{max}^{sp} and T_{max}^{su}. Early and mid-growing season (e.g., spring and early summer) warming tends to trigger regional droughts (Supplementary Fig. S14-S16), which can exert strong control on vegetation growth and even cause tree mortality in the temperate NH and some parts of the cold NH[28,30–32]. Nevertheless, the emergence of a positive response of $NDVI_{GS}$ to T_{max} in autumn may reflect alleviation of water stress on photosynthetic activity in that period (Figs 1and 4, Supplementary Figs S1, S14)[33], which is confirmed by a generally negative correlation between $NDVI_{GS}$ and the autumn WAI (Fig. 1). Consequently, alleviation of water limitations in autumn (Fig. 4, Supplementary Fig. S14) results in a generally positive correlation between the TRI and T_{max}^{au} in ~49% of the temperate NH except in portions of arid regions (e.g., the central U.S.A.). By contrast, a predominantly (~60–70%) negative correlation exists between the TRI and T_{max}^{sp} and T_{max}^{su} (Fig. 1, Supplementary Figs S1, S13). These factors also lead to a conversion from a generally (~55–81%) negative correlation between γ_{GPP} and T_{max}^{sp} and T_{max}^{su} to a positive correlation (in ~57–67% of the temperate NH) between γ_{GPP} and T_{max}^{au} in the temperate NH (Supplementary Fig. S8a–c).

The positive responses of the AVG to variations in the mean nighttime temperatures T_{min}^{sp} and T_{min}^{su} in parts of NH are most likely attributable to the reported compensation effects of nocturnal warming[34]. However, the shifting responses of the AVG to T_{min}^{sp} and T_{min}^{su} in arid and temperate arid regions (Fig. 1, Supplementary Fig. S1, S3 and Table S2) imply that the compensation effects of nocturnal warming on vegetation growth might be seasonally and spatially dependent and are likely modified by other bio-physical factors, such as water conditions (Fig. 4) and plant functional types[35]. In contrast to the ambiguous relationships between the AVG and T_{min}^{sp} and T_{min}^{su}, there is a pervasive negative response of the AVG, from the perspective of $NDVI_{GS}$ and GPP_{GS}, to T_{min}^{au} across most of the temperate and cold NH except in certain mountainous regions (e.g., the Rocky Mountains in western North America). The dominant effect of autumn nocturnal warming on NH vegetation growth may be enhanced plant respiration, which consequently leads to autumn carbon loss[36]. However, the TRI data indicate a persistent positive rather than negative correlation with T_{min}^{au} (Fig. 1). In addition to enhanced whole-plant respiration, warmer autumn (both day and night) temperatures may reactivate cambial activity[37]. Combined with alleviation of water limitations (Fig. 4, Supplementary Figs S14-S17), these process may partially explain the observed widespread positive correlation between the TRI and T_{min}^{au} in the temperate NH. Overall, the observed divergent responses of AVG to seasonal T_{min} in portions of the NH are to some degree attributable to the water-mediated counterbalancing effects of T_{min} on vegetation growth and respiration[34,38,39].

In summary, remote sensing retrievals, empirical up-scaling measurements from FLUXNET, and tree growth data consistently indicate a possible water-mediated divergent response of vegetation activity to seasonal VDNC, especially in temperate regions and boreal regions with dry summers in the NH. Our research provides new insights into the seasonally divergent responses of the AVG to the seasonal asymmetry in the VDNC and reinforces the idea that the projected intensification in the asymmetry in the seasonal VDNC under continued global warming and increasing climate extremes[40] may have strong, spatially variable effects on vegetation growth and carbon dynamics in the NH, with associated changes in regional ecosystem services, the terrestrial carbon cycle, and global climate feedbacks.

Methods

Remote sensing data and up-scaled GPP. We used three types of data to investigate how AVG (i.e., vegetation growth during the growing season) responded to the mean seasonal VDNC: the satellite-derived AVHRR/GIMMS Normalized Difference Vegetation Index (NDVI, specifically version NDVI3g)[18,19], the satellite-derived Fraction of Absorbed Photosynthetically Active Radiation (FAPAR)[20], and FLUXNET-based up-scaled gross primary production (GPP) data[21]. The data featured a spatial resolution of 0.5° × 0.5° and a monthly temporal resolution for 1982–2008. Pixels with a multi-year mean annual NDVI value <0.10 were masked in our study.

Tree ring data. In total, 149 standard TRI chronologies from the mid- and high-latitude NH were used to investigate the interannual responses of tree growth to the seasonal VDNC. Standard TRI chronologies were built following the standard procedures of dendrochronology[41], including fitting a curve to the raw ring-width series and then dividing each ring-width value by the corresponding curve value to generate a series of growth indices. Of these chronologies, 136 were obtained from the International Tree-Ring Data Bank (ITRDB, http://www.ncdc.noaa.gov/data-access/paleoclimatology-data/datasets/tree-ring) based on four criteria: 1) intact records of latitude, longitude, elevation, species and sample depth; 2) the chronologies cover at least 1950–1998 or extend to more recent times (i.e., early 21st century); 3) the sample depth for each site-year is greater than 10; and 4) the altitude of the sample site is less than the 90th percentile of the elevation distribution of the surrounding 0.5° × 0.5° region based on the GTOPO30 dataset (with ~1 km resolution, available from U.S. Geological Survey, https://lta.cr.usgs.gov/GTOPO30) to match the regional vegetation growth patterns and avoid site-specific representations. Our research group provided another 13 standard chronologies from northern China. Our chronologies satisfy the four criteria listed above (see Table S4 for details).

Climate data. Monthly mean maximum (T_{max}, averaging daily maximum temperature) and mean minimum temperature (T_{min}, averaging daily minimum temperature) at a spatial resolution of 0.5° were obtained from the newly updated CRU TS 3.22 dataset (http://www.cru.uea.ac.uk/). The seasonal (in detail see section of sensitivity

test) mean T_{max} and T_{min} were then calculated by averaging the monthly mean climate data. The seasonal mean T_{max} and T_{min} are used in this study to represent the general climate conditions of seasonal mean daytime and nighttime temperature[3], respectively. Remotely sensed soil moisture data with a daily resolution for the period 1978–2013 were obtained from the Essential Climate Variable Soil Moisture dataset (ECV SM 02.0) (http://www.esa-soilmoisture-cci.org/). These data were produced following the method described by Liu *et al.* (2011) and Liu *et al.* (2012)[42,43], representing surface soil moisture with a global coverage and spatial resolution of 0.25°. We then resampled this surface soil moisture data to a spatial resolution of 0.5° × 0.5°. Unfortunately, the soil moisture data were not continuous during 1982–2008, and only pixels with at least 19 years of data between 1982 and 2008 were retained.

Water deficit and WAI. The monthly water deficit was estimated using a simple water balance equation:

$WD_i = PRE_i - PET_i$where WD_i, PRE_i, and PET_i are the water deficit (positive values indicate water surpluses), precipitation and potential evapotranspiration in month *i*. The potential evapotranspiration is calculated using Thornthwaite's equation[44]. Then, the total seasonal water deficit is calculated by summing the monthly *WD* values. Negative values express the degree of dryness; the more negative the value, the more intense the water limitation. In our study, the monthly *WAI* was calculated based on the water balance equation proposed by Kleidon and Heimann (1998)[45] and was used to represent the soil moisture conditions.

Statistical analysis. Spearman partial correlation and ridge regression were performed to investigate the responses of vegetation activity in the mid- and high-latitude NH to the mean seasonal VDNC. The interannual sensitivity of vegetation growth to IAV in the seasonal VDNC was evaluated using the ridge regression coefficients. Ridge regression has been demonstrated to be an effective method for addressing collinearity in multivariate regression[46]. The probability density function (PDF) of the Spearman partial correlation coefficients between the seasonal VDNC and the IAV in the AVG was estimated for seven major climate zones (as defined by the Köppen–Geiger climate classification[47]), including arid (RegAR, grouping of BWk, BWh, BSk, and BSh), warm temperate humid (RegTH, grouping of Cfa, Cfb and Cfc), warm temperate arid (RegTA, grouping of Csa, Csb, Csc, Cwa, Cwb, and Cwc), cold humid (RegAH, grouping of Dfa, Dfb, Dfc, and Dfd), cold summer dry (RegAS, grouping of Dsa, Dsb, Dsc, and Dsd), cold winter dry (RegAW, grouping of Dwa, Dwb, Dwc, Dwd) and polar tundra (RegET). Prior to performing the Spearman partial correlation and ridge regression analyses, all variables (i.e., NDVI, FAPAR, GPP, TRI and the climate variables) were detrended using a linear function. The statistical analyses and figure creation were performed using the MATLAB software package (R2012b).

Sensitivity test. In this study, we attempted to define the seasons (spring, summer, and autumn) in a manner that is consistent across the mid- and high-latitude NH. Notably, three different definitions of seasons were used in our study to verify the robustness of our conclusions relative to the arbitrary definitions of vegetation growth seasons in the mid- and high-latitude NH. The three definitions are as follows:

Definition 1: spring: April-May; summer: June-August; autumn: September-October

Definition 2: spring: April-May; summer: June-August; autumn: September

Definition 3: spring: May; summer: June-August; autumn: September-October

We then performed the same analyses for the three different season definitions. The results of Definition 1 are presented in the main text, and the results of the other two definitions are presented in the supplementary materials.

References

1. Myneni, R., Keeling, C., Tucker, C., Asrar, G. & Nemani, R. Increased plant-growth in the northern high-latitudes from 1981 to 1991. *Nature* **386**, 698–702 (1997).
2. Nemani, R. R. *et al.* Climate-driven increases in global terrestrial net primary production from 1982 to 1999. *Science* **300**, 1560–1563 (2003).
3. Peng, S. *et al.* Asymmetric effects of daytime and night-time warming on Northern Hemisphere vegetation. *Nature* **501,** 88–92 (2013).
4. Keeling, C., Chin, J. & Whorf, T. Increased activity of northern vegetation inferred from atmospheric CO_2 measurements. *Nature* **382,** 146–149 (1996).
5. Reay, D. S., Dentener, F., Smith, P., Grace, J. & Feely, R. A. Global nitrogen deposition and carbon sinks. *Nature Geoscience* **1,** 430–437 (2008).
6. Piao, S. *et al.* Evidence for a weakening relationship between interannual temperature variability and northern vegetation activity. *Nature Communications* **5,** doi: 10.1038/ncomms6018 (2014).
7. Braganza, K., Karoly, D. J. & Arblaster, J. Diurnal temperature range as an index of global climate change during the twentieth century. *Geophysical Research Letters* **31,** doi: 10.1029/2004GL019998, L13217 (2004).
8. Easterling, D. R. *et al.* Maximum and minimum temperature trends for the globe. *Science* **277,** 364–367 (1997).
9. Karl, T. *et al.* A new perspective on recent global warming: Asymmetric trends of daily maximum and minimum temperature. *Bulletin of the American Meteorological Society* **74,** 1007–1023 (1993).
10. IPCC. Climate change 2013: The physical science basis. *Contribution of working group I to the fifth assessment report of the intergovernmental panel on climate change*. 1535 pp (Cambridge, United Kingdom and Now York, NY, USA, 2013).
11. Xu, L. *et al.* Temperature and vegetation seasonality diminishment over northern lands. *Nature Climate Change* **3,** 581–586 (2013).
12. Sun, D., Kafatos, M., Pinker, R. T. & Easterling, D. R. Seasonal variations in diurnal temperature range from satellites and surface observations. *IEEE Transactions on Geoscience and Remote Sensing* **44,** 2779–2785 (2006).
13. Betts, A. K., Desjardins, R., Worth, D. & Cerkowniak, D. Impact of land use change on the diurnal cycle climate of the Canadian Prairies. *Journal of Geophysical Research: Atmospheres* **118,** doi: 10.1002/2013jd020717 (2013).
14. Chou, C. *et al.* Increase in the range between wet and dry season precipitation. *Nature Geoscience* **6,** 263–267 (2013).
15. Bonan, G. B. Forests and Climate Change: Forcings, Feedbacks, and the Climate Benefits of Forests. *Science* **320,** 1444–1449 (2008).
16. Angert, A. *et al.* Drier summers cancel out the CO_2 uptake enhancement induced by warmer springs. *Proceedings of the National Academy of Sciences of the United States of America* **102,** 10823–10827 (2005).

17. Wang, X. *et al.* Spring temperature change and its implication in the change of vegetation growth in North America from 1982 to 2006. *Proceedings of the National Academy of Sciences of the United States of America* **108,** 1240–1245 (2011).
18. Tucker, C. J. *et al.* An extended AVHRR 8-km NDVI dataset compatible with MODIS and SPOT vegetation NDVI data. *International Journal of Remote Sensing* **26,** 4485–4498 (2005).
19. Pinzon, J. E. & Tucker, C. J. A non-stationary 1981–2012 AVHRR NDVI3g time series. *Remote Sensing* **6,** 6929–6960 (2014).
20. Zhu, Z. *et al.* Global data sets of vegetation leaf area index (LAI) 3 g and Fraction of Photosynthetically Active Radiation (FPAR) 3 g derived from Global Inventory Modeling and Mapping Studies (GIMMS) Normalized Difference Vegetation Index (NDVI3g) for the period 1981 to 2011. *Remote Sensing* **5,** 927–948 (2013).
21. Jung, M. *et al.* Global patterns of land-atmosphere fluxes of carbon dioxide, latent heat, and sensible heat derived from eddy covariance, satellite, and meteorological observations. *Journal of Geophysical Research: Biogeosciences* **116,** G00J07, doi: 10.1029/2010JG001566 (2011).
22. Beer, C. *et al.* Terrestrial gross carbon dioxide uptake: global distribution and covariation with climate. *Science* **329,** 834–838 (2010).
23. Lucht, W. *et al.* Climatic control of the high-latitude vegetation greening trend and Pinatubo effect. *Science* **296,** 1687–1689 (2002).
24. Zhao, M. & Running, S. W. Drought-induced reduction in global terrestrial net primary production from 2000 through 2009. *Science* **329,** 940–943 (2010).
25. Barber, V. A., Juday, G. P. & Finney, B. P. Reduced growth of Alaskan white spruce in the twentieth century from temperature-induced drought stress. *Nature* **405,** 668–673 (2000).
26. Zhang, X., Tarpley, D. & Sullivan, J. T. Diverse responses of vegetation phenology to a warming climate. *Geophysical Research Letters* **34,** L19405, doi: 10.1029/2007GL031447 (2007).
27. Turnbull, M., Murthy, R. & Griffin, K. The relative impacts of daytime and night-time warming on photosynthetic capacity in Populus deltoides. *Plant, Cell & Environment* **25,** 1729–1737 (2002).
28. Liu, H. *et al.* Rapid warming accelerates tree growth decline in semi-arid forests of Inner Asia. *Global Change Biology* **19,** 2500–2510 (2013).
29. Breshears, D. D. *et al.* Regional vegetation die-off in response to global-change-type drought. *Proceedings of the National Academy of Sciences of the United States of America* **102,** 15144–15148 (2005).
30. Allen, C. D. *et al.* A global overview of drought and heat-induced tree mortality reveals emerging climate change risks for forests. *Forest Ecology and Management* **259,** 660–684 (2010).
31. Williams, A. P. *et al.* Temperature as a potent driver of regional forest drought stress and tree mortality. *Nature Climate Change* **3,** 292–297 (2013).
32. Peng, C. *et al.* A drought-induced pervasive increase in tree mortality across Canada's boreal forests. *Nature Climate Change* **1,** 467–471 (2011).
33. Vaz, M. *et al.* Drought-induced photosynthetic inhibition and autumn recovery in two Mediterranean oak species (*Quercus ilex* and *Quercus suber*). *Tree Physiology* **30,** 946–956 (2010).
34. Wan, S., Xia, J., Liu, W. & Niu, S. Photosynthetic overcompensation under nocturnal warming enhances grassland carbon sequestration. *Ecology* **90,** 2700–2710 (2009).
35. Alward, R. D., Detling, J. K. & Milchunas, D. G. Grassland vegetation changes and nocturnal global warming. *Science* **283,** 229–231 (1999).
36. Piao, S. *et al.* Net carbon dioxide losses of northern ecosystems in response to autumn warming. *Nature* **451,** 49–52 (2008).
37. De Luis, M., Gricar, J., Cufar, K. & Raventos, J. Seasonal dynamics of wood formation in Pinus halepensis from dry and semi-arid ecosystems in Spain. *Iawa Journal* **28,** 389–404 (2007).
38. Xia, J., Han, Y., Zhang, Z. & Wan, S. Effects of diurnal warming on soil respiration are not equal to the summed effects of day and night warming in a temperate steppe. *Biogeosciences* **6,** 1361–1370 (2009).
39. Still, C. Biogeochemistry: As different as night and day. *Nature* 501, 39–40 (2013).
40. Reichstein, M. *et al.* Climate extremes and the carbon cycle. *Nature* **500,** 287–295 (2013).
41. Cook, E. R. & Kairiukstis, L. A. *Methods of dendrochronology: applications in the environmental sciences*. (Springer Science & Business Media, 1990).
42. Liu, Y. *et al.* Trend-preserving blending of passive and active microwave soil moisture retrievals. *Remote Sensing of Environment* **123,** 280–297 (2012).
43. Liu, Y. *et al.* Developing an improved soil moisture dataset by blending passive and active microwave satellite-based retrievals. *Hydrology and Earth System Sciences* **15,** 425–436 (2011).
44. Thornthwaite, C. W. An approach toward a rational classification of climate. *Geographical Review* **38,** 55–94 (1948).
45. Kleidon, A. & Heimann, M. A method of determining rooting depth from a terrestrial biosphere model and its impacts on the global water and carbon cycle. *Global Change Biology* **4,** 275–286 (1998).
46. Hoerl, A. E. & Kennard, R. W. Ridge regression: Biased estimation for nonorthogonal problems. *Technometrics* **12,** 55–67 (1970).
47. Kottek, M., Grieser, J., Beck, C., Rudolf, B. & Rubel, F. World map of the Koppen-Geiger climate classification updated. *Meteorologische Zeitschrift* **15,** 259–264 (2006).

Acknowledgements

The digital elevation model data, GTOPO30, was obtained from the U.S. Geological Survey. X.L. is supported by the National Natural Science Foundation of China (NSFC No. 41390462 and 41130640). X.W. is supported by the National Natural Science Foundation of China (NSFC No. 41571038) and the Fundamental Research Funds for the Central Universities (Grant No. 2014NT40). H.L. is financially supported by the National Natural Science Foundation of China (NSFC No. 41530747).

Author Contributions

X.W. conceived the idea, designed the paper, performed the numerical analysis and led the interpretation of the results. H.L. and E.L. contributed parts of the tree growth increment data. X.L., P.B. and H.L. assisted with selection of the main results for presentation. X.W., H.L., X.L., E.L., P.B. and Y.H. contributed to interpreting the results and writing the paper.

Additional Information

Supplementary information accompanies this paper at http://www.nature.com/srep

Competing financial interests: The authors declare no competing financial interests.

How to cite this article: Wu, X. *et al.* Seasonal divergence in the interannual responses of Northern Hemisphere vegetation activity to variations in diurnal climate. *Sci. Rep.* **6**, 19000; doi: 10.1038/srep19000 (2016).